Measurement of the 240Pu(n, f) cross-section at the CERN n_TOF facility: First results from experimental area II (EAR-2)

(n_TOF Collaboration) Stamatopoulos, A.; ...; Žugec, Petar; ...; Bosnar, Damir; ...; Wright, T.

EPJ Web of Conferences **146**, 04030 (2017) DOI: 10.1051/epjconf/201714604030
ND2016

Measurement of the ^{240}Pu(n,f) cross-section at the CERN n_TOF facility: First results from experimental area II (EAR-2)

A. Stamatopoulos[1,a], A. Tsinganis[1,2], N. Colonna[3], R. Vlastou[1], M. Kokkoris[1], P. Schillebeeckx[4], A. Plompen[4], J. Heyse[4], P. Žugec[6], M. Barbagallo[3], M. Calviani[2], E. Berthoumieux[5], E. Chiaveri[2], O. Aberle[2], J. Andrzejewski[7], L. Audouin[8], V. Bécares[9], M. Bacak[10], J. Balibrea[9], S. Barros[11], F. Bečvář[12], C. Beinrucker[13], F. Belloni[5], J. Billowes[14], V. Boccone[2], D. Bosnar[6], M. Brugger[2], M. Caamaño[15], F. Calviño[16], D. Cano-Ott[9], F. Cerutti[2], G. Cortés[16], M.A. Cortés-Giraldo[17], L. Cosentino[18], L.A. Damone[4,19], K. Deo[20], M. Diakaki[5,1], C. Domingo-Pardo[21], R. Dressler[22], E. Dupont[5], I. Durán[15], B. Fernández-Domínguez[15], A. Ferrari[2], P. Ferreira[11], P. Finocchiaro[19], R.J.W. Frost[14], V. Furman[23], K. Göbel[13], M.B. Gómez-Hornillos[16], A.R. García[9], I. Gheorghe[24], T. Glodariu[24], I.F. Gonçalves[11], E. González[9], A. Goverdovski[25], E. Griesmayer[10], C. Guerrero[17], F. Gunsing[5,2], H. Harada[26], T. Heftrich[13], S. Heinitz[22], A. Hernández-Prieto[2,16], D.G. Jenkins[27], E. Jericha[10], F. Käppeler[28], Y. Kadi[2], T. Katabuchi[29], P. Kavrigin[10], V. Ketlerov[25], V. Khryachkov[25], A. Kimura[26], N. Kivel[22], M. Krtička[12], E. Leal-Cidoncha[15], C. Lederer[13,30], H. Leeb[10], J. Lerendegui-Marco[17], M. Licata[31,32], S. Lo Meo[31,33], R. Losito[2], D. Macina[2], J. Marganiec[2], T. Martínez[9], C. Massimi[31,32], P. Mastinu[34], M. Mastromarco[3], F. Matteucci[35,36], E. Mendoza[9], A. Mengoni[33], P.M. Milazzo[35], F. Mingrone[31], M. Mirea[24], S. Montesano[2], A. Musumarra[18,37], R. Nolte[38], F.R. Palomo-Pinto[17], C. Paradela[15], N. Patronis[39], A. Pavlik[40], J. Perkowski[7], J.I. Porras[2,41], J. Praena[17], J.M. Quesada[17], T. Rauscher[42,43], R. Reifarth[13], A. Riego-Perez[16], M. Robles[15], C. Rubbia[2], J.A. Ryan[14], M. Sabaté-Gilarte[2,17], A. Saxena[20], S. Schmidt[13], D. Schumann[22], P. Sedyshev[23], A.G. Smith[14], S.V. Suryanarayana[20], G. Tagliente[3], J.L. Tain[21], A. Tarifeño-Saldivia[21], L. Tassan-Got[8], S. Valenta[12], G. Vannini[31,32], V. Variale[3], P. Vaz[11], A. Ventura[31], V. Vlachoudis[2], A. Wallner[44], S. Warren[14], M. Weigand[13], C. Weiss[2,10], and T. Wright[14]

[1] National Technical University of Athens (NTUA), Greece
[2] European Organisation for Nuclear Research (CERN), Geneva, Switzerland
[3] Istituto Nazionale di Fisica Nucleare, Sezione di Bari, Italy
[4] European Commission JRC, Institute for Reference Materials and Measurements, Retieseweg 111, 2440 Geel, Belgium
[5] Commissariaté l'énergie Atomique (CEA) Saclay – Irfu, Gif-sur-Yvette, France
[6] Department of Physics, Faculty of Science, University of Zagreb, Croatia
[7] University of Lodz, Poland
[8] Institut de Physique Nucléaire, CNRS-IN2P3, Univ. Paris-Sud, Université Paris-Saclay, 91406 Orsay Cedex, France
[9] Centro de Investigaciones Energeticas Medioambientales y Tecnológicas (CIEMAT), Spain
[10] Technische Universität Wien, Austria
[11] Instituto Superior Técnico, Lisbon, Portugal
[12] Charles University, Prague, Czech Republic
[13] Goethe University Frankfurt, Germany
[14] University of Manchester, UK
[15] University of Santiago de Compostela, Spain
[16] Universitat Politécnica de Catalunya, Spain
[17] Universidad de Sevilla, Spain
[18] INFN Laboratori Nazionali del Sud, Catania, Italy
[19] Dipartimento di Fisica, Université degli Studi di Bari, Italy
[20] Bhabha Atomic Research Centre (BARC), India
[21] Instituto de Física Corpuscular, Universidad de Valencia, Spain
[22] Paul Scherrer Institut (PSI), Villingen, Switzerland
[23] Joint Institute for Nuclear Research (JINR), Dubna, Russia
[24] Horia Hulubei National Institute of Physics and Nuclear Engineering, Romania
[25] Institute of Physics and Power Engineering (IPPE), Obninsk, Russia
[26] Japan Atomic Energy Agency (JAEA), Tokai-mura, Japan
[27] University of York, UK
[28] Karlsruhe Institute of Technology, Campus North, IKP, 76021 Karlsruhe, Germany
[29] Tokyo Institute of Technology, Japan
[30] School of Physics and Astronomy, University of Edinburgh, UK
[31] Istituto Nazionale di Fisica Nucleare, Sezione di Bologna, Italy
[32] Dipartimento di Fisica e Astronomia, Université di Bologna, Italy
[33] Agenzia nazionale per le nuove tecnologie (ENEA), Bologna, Italy

[34] Istituto Nazionale di Fisica Nucleare, Sezione di Legnaro, Italy
[35] Istituto Nazionale di Fisica Nucleare, Sezione di Trieste, Italy
[36] Dipartimento di Astronomia, Université di Trieste, Italy
[37] Dipartimento di Fisica e Astronomia, Université di Catania, Italy
[38] Physikalisch-Technische Bundesanstalt (PTB), Bundesallee 100, 38116 Braunschweig, Germany
[39] University of Ioannina, Greece
[40] University of Vienna, Faculty of Physics, Vienna, Austria
[41] University of Granada, Spain
[42] Centre for Astrophysics Research, University of Hertfordshire, UK
[43] Department of Physics, University of Basel, Switzerland
[44] Australian National University, Canberra, Australia

Abstract. The accurate knowledge of the neutron-induced fission cross-sections of actinides and other isotopes involved in the nuclear fuel cycle is essential for the design of advanced nuclear systems, such as Generation-IV nuclear reactors. Such experimental data can also provide the necessary feedback for the adjustment of nuclear model parameters used in the evaluation process, resulting in the further development of nuclear fission models. In the present work, the ^{240}Pu(n,f) cross-section was measured at CERN's n_TOF facility relative to the well-known ^{235}U(n,f) cross section, over a wide range of neutron energies, from meV to almost MeV, using the time-of-flight technique and a set-up based on Micromegas detectors. This measurement was the first experiment to be performed at n_TOF's new experimental area (EAR-2), which offers a significantly higher neutron flux compared to the already existing experimental area (EAR-1). Preliminary results as well as the experimental procedure, including a description of the facility and the data handling and analysis, are presented.

1. Introduction

The optimum design and development of advanced nuclear systems requires the accurate knowledge of neutron induced fission cross sections of plutonium isotopes and other minor actinides [1,2]. More specifically, the ^{240}Pu isotope is included in the Nuclear Energy Agency's (NEA) High Priority Request List (HPRL) [3] as well as in the NEMEA-4 meeting proceedings [4]. Requested target accuracies are in the order of 1.6%–11.8% for the energy region 0.454 keV–6.07 MeV compared to the presently reported 3.9%–21.6%. The previous experiment carried out at the n_TOF's Experimental Area 1 (EAR-1), was unsuccessful due to detector deterioration caused by the high alpha activity of the ^{240}Pu samples in addition to the long period needed to complete the measurement [5], therefore the neutron induced fission cross section had to be remeasured in the newly constructed experimental area EAR-2, which offers a higher background suppression and a significantly higher instantaneous neutron flux, thus reducing the time needed to complete the measurement. Similar recent measurements have also been performed at GNEIS [6], LANSCE [7] and IRMM [8].

2. Experimental setup

2.1. The n_TOF facility

The measurement was performed at CERN's n_TOF facility [9–11], in the newly commissioned experimental area EAR-2 [12]. The neutrons are produced by spallation, occurring when a 20 GeV/c pulsed proton beam, delivered by CERN's Proton Synchrotron [13], impinges on a 40 cm in length and 60 cm in diameter lead block, resulting in a neutron energy spectrum that spans from the meV to the GeV region. The proton pulse has a duration of 6 ns RMS, a maximum repetition rate of 1 pulse per 1.2 s and nominally carries 7×10^{12} protons. The 1.3 ton lead target is surrounded by a 1 cm-thick layer of water as well as an additional 4 cm-thick layer of borated water ($H_20 + 1.28\% H_3BO_3$, fraction in mass) which act as coolant and neutron moderator respectively. Following the target in the beam direction, a beam pipe of 182.3 m leads to the first experimental area EAR-1. The new experimental area EAR-2 is located 18.16 m above the spallation target, perpendicular to the beam direction, offering a $25-30$ times higher flux [14] and approximately 10 times shorter time of flights compared to the existing area. The high instantaneous flux, combined with the wide white neutron spectrum (from thermal energies to the MeV region), leads to the relative suppression of the contribution originating from the high intrinsic $\alpha-$background of the samples, thus allowing for accurate measurements below the fission threshold, where the fission cross section is low.

2.2. Samples

Three high purity (99.89% atomic abundance) plutonium dioxide (PuO_2) samples, prepared at IRMM (Belgium) [15] for the previous measurement in EAR-1, were used having a total ^{240}Pu mass of 2.288 mg (~ 100 μgr/cm^2 per sample) and a total α-activity of 19.219 MBq. The oxide material was electro-deposited on a 250 μm-thick aluminum backing with a diameter of 5 cm, while the deposit itself had a diameter of 3 cm. In addition to the plutonium samples, two targets were used as reference: a ^{235}U and a ^{238}U, with a mass of ~ 0.6 mg and $\sim$0.8 mg respectively. The impurities found in the samples, mainly ^{239}Pu, have a non-negligible contribution in the obtained yields below 1 keV, which was thoroughly taken into account in the analysis.

2.3. Detectors

The measurement was carried out using a set-up based on the extremely compact, low mass Micromegas (Micro-Mesh Gaseous Structure) gaseous detector [16–18]. Its volume is divided into two parts by a thin, 35 μm pitched micro-mesh: a drift region (5 mm) and a narrow amplification region (50 μm), in which a high

[a] e-mail: athanasios.stamatopoulos@cern.ch

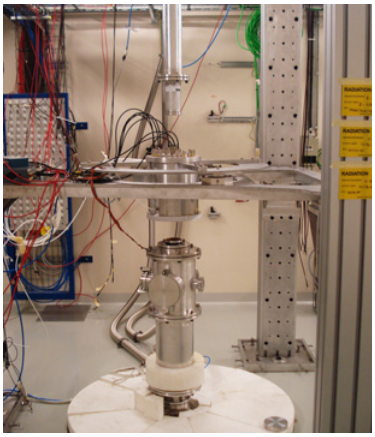

Figure 1. The fission chamber, which housed the detectors and samples, as seen inside the experimental area EAR-2, in the middle of the picture. The neutron beam was delivered vertically from bottom to top.

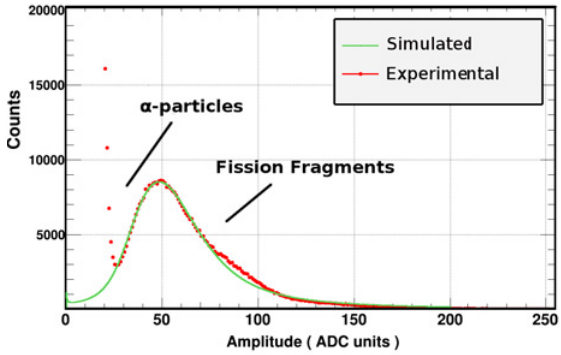

Figure 2. Experimental (red points) and simulated (green line) typical pulse height spectra for ^{240}Pu. The direct simulated output is calibrated and convoluted with the detector's response function.

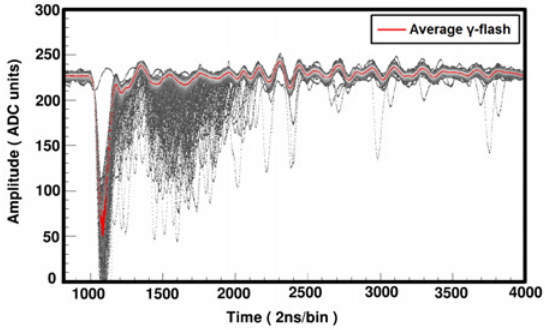

Figure 3. Typical average γ-flash (red) and raw γ-flash pulses (gray scale) for ^{240}Pu. During the extraction of the average, the fission signals are rejected. The average γ-flash shape is typically calculated from one thousand raw signals.

electric field causes an avalanche multiplication. Typical operating electric fields are $\sim$ 1 kV/cm and $\sim$ 100 kV/cm respectively depending on the gas, which in this case was a mixture of Ar:CF_4:isoC_4H_{10} (88:10:2) at atmospheric pressure and room temperature. The detector set-up consisted of 6 similar detectors in total (3 for the plutonium samples, 2 for the uranium samples and 1 for monitoring possible proton recoils from the surrounding materials), all of which were housed in a cylindrical aluminum chamber as shown in Fig. 1.

2.4. Data acquisition

The analogue detector signals were recorded using a high performance digital acquisition system [19], operating at a 500 MHz sampling rate with a resolution of 8 bits. To minimize the amount of data recorded during acquisition, a zero-suppression algorithm was applied.

3. Data analysis

An offline pulse shape analysis routine [20] parses the raw data, determining, among others, the amplitude and the position in time of every recorded signal. During the experiment, beam-off data was obtained in order to measure the contribution of the α-activity as well as spontaneous fission. Monte Carlo simulations were also performed, using the general purpose code FLUKA [21,22] to study the behavior of the detectors. More specifically, the pulse height spectra of α-particles and fission fragments were reconstructed for all detectors, making possible both the estimation of the detection efficiency and the determination of the correction for the signal amplitude threshold, which was found to be in the order of 10%. A typical experimental pulse height spectrum along with the simulated one, is shown in Fig. 2.

The proton interaction with the lead target, apart from the neutron production, results in the generation of prompt γ-rays and relativistic particles, that reach the experimental hall at (nearly) the speed of light. This burst of particles is commonly referred to in literature as "γ-flash". The γ-flash results in the formation of a high amplitude pulse, comparable to the fission signals, which lasts a few hundreds of ns and is followed by a baseline oscillation in times of flight that correspond to energies in the MeV region. To mitigate this effect, an average γ-flash shape is derived for every detector, which is subtracted individually from each γ-flash pulse, during the offline raw data processing. A typical average γ-flash is shown in Fig. 3.

The $^{240}Pu(n,f)$ cross section was calculated using the reference reactions $^{235}U(n,f)$ and $^{238}U(n,f)$ for flux normalisation purposes. The detector dead time, as well as the background contribution due to sample impurities were taken into account during the analysis. The final experimental cross section was derived from the weighted average between the three individual cross sections, calculated for each plutonium target. Preliminary results are shown in Fig. 4 for the energy range 6 keV-35 keV, while resonances can be resolved up to a few tens of keV. The present preliminary data comparison with the latest ENDF/B-VII.1 library [23,24], reveals that the aforementioned resonances are not included in the evaluations, as Fig. 4 demonstrates. Resonance analysis is planned to be performed, using R-matrix calculations, to characterize the resolved resonances.

In the energy range above 35 keV, data has been obtained up to at least several MeV. Specifically in the sub-threshold region between 100 keV and 600 keV, the shape of the extracted cross section is in general agreement with the ENDF/B-VII.1 evaluations, as shown in Fig. 5.

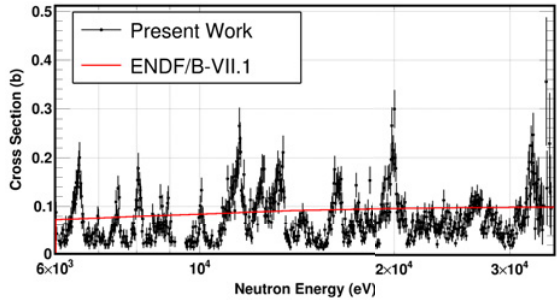

Figure 4. Comparison between present data (black points) and ENDF/B-VII.1 evaluation (red line) in the energy range 6 keV-35 keV. Clusters of resonances, that are attributed to transitions between Class-I and Class-II states are visible, while resonances can be resolved up to a few tens of keV. Data is shown using a binning of 2000 bins per energy decade.

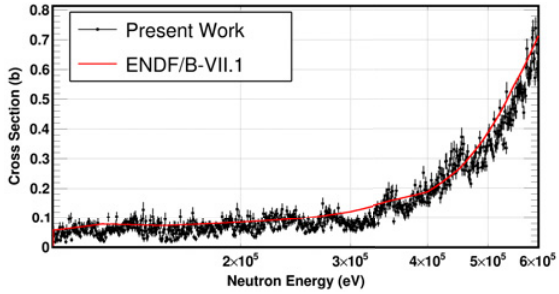

Figure 5. Comparison between present data (black points) and ENDF/B-VII.1 evaluation (red line) in the energy range 100 keV–600 keV. Data is shown using a binning of 2000 bins per energy decade.

Resonance-like structures are also observed, which are attributed to high transition states. Above 1 MeV, the non optimized sample mass caused a high counting rate which affects the normalisation, therefore analysis is still ongoing.

4. Conclusion

The ^{240}Pu neutron induced fission cross section, is the first measurement to be performed in the newly commissioned experimental area EAR-2, at CERN's n_TOF facility. Data was obtained over a wide energy range that spans from thermal energies up to at least a few MeV. Most remarkably, data in the sub-threshold region, shows clear resonance structures which are not included in the evaluated libraries. R-matrix calculations will be performed to characterize these structures. In the MeV region, preliminary data shows a general agreement with the evaluations, yet further analysis is ongoing. The higher instantaneous flux along with the stronger background suppression, compared to the existing experimental area EAR-1, are deemed crucial to the success of this measurement, following which additional measurements are planned that include the study of short-lived and rare isotopes such as ^{230}Th, ^{232}U, $^{238,241}Pu$ and ^{244}Cm.

The authors would like to acknowledge the support of the European Commission under the ANDES, ERINDA and CHANDA projects (7th Framework Programme).

References

[1] https://www.gen-4.org/gif/jcms/c_9260/public
[2] https://www.ifnec.org/ifnec/
[3] https://www.oecd-nea.org/dbdata/hprl/hprl.pl
[4] M. Salvatores et al., NEMEA-4 proceedings, JRC 42917
[5] A. Tsinganis et al., Deliverable 1.5 of the ANDES project, Ch. 3, JRC85144 (2013)
[6] A.B. Laptev et al., Nuclear Physics A **734**, E45–E48 (2004)
[7] F. Tovesson et al., Physical Review C **79**, 014613 (2009)
[8] P. Salvador-Castiñeira et al., Physics Procedia **64**, 177–182 (2015)
[9] U. Abbondanno et al., CERN-SL-2002-053 ECT
[10] C. Guerrero et al., Eur. Phys. J. A **49**, 1–15 (2013)
[11] E. Berthoumieux et al., CERN-nTOF-PUB-2013-001
[12] C. Weiéy et al., NIM A **799**, 90–98 (2015)
[13] J.P. Burnet et al., CERN-2011-004, 2011
[14] A. Tsinganis et al., 14th International Conference on Nuclear Reaction Mechanisms Proceedings, p. 21–26 (2016)
[15] G. Sibbens et al., J. Radioanal. Nucl. Ch. **299**, 1093–1098 (2014)
[16] Y. Giomataris et al., NIM A **376**(1), 29–35 (1996)
[17] Y. Giomataris, NIM A **419**, 230–250 (1998)
[18] Y. Giomataris, ICFA Instrum. Bul., 19
[19] U. Abbondanno et al., NIM A **538**, 692–702 (2005)
[20] P. Žugec et al., NIM A **812**, 134–144 (2016)
[21] A. Ferrari et al., Nuclear Data Sheets **120**, 211–214 (2014)
[22] A. Ferrari et al., CERN-2005-010 (2005)
[23] https://www-nds.iaea.org/exfor/endf.htm
[24] M.B. Chadwick et al., NDS **112**, 2887–2996 (2011)